

Machine Generalize Learning in Agent-Based Models: Going Beyond Surrogate Models for Calibration in ABMs

Sima Najafzadehkhoie

George G. Vega Yon

Bernardo Modenesi

Derek S. Meyer

August 26, 2025

1 Introduction

Agent-based models (ABMs) are increasingly valuable tools for understanding complex systems, particularly in public health contexts where simulating interactions among individuals can reveal important epidemiological dynamics. However, calibrating ABMs—identifying parameter values that produce realistic model outputs—is typically computationally intensive, posing a significant challenge for timely public health responses. This paper introduces a machine learning (ML) algorithm designed to address these calibration challenges effectively. By leveraging training data generated directly from the ABM and performing supervised learning with it, our approach not only improves calibration accuracy but also significantly reduces the computational burden.

Although various methods integrate ML with ABMs^{1,6}, most, if not all, are utilized to create mappings from observed parameters to realized data—often referred to as surrogate models. In contrast, our method generates the inverse mapping: from observed data back to the parameters.

To demonstrate the effectiveness of our method, we use a susceptible-infectious-recovered (SIR) ABM as an illustrative example. The proposed ML-based calibration method is compared with Approximate Bayesian Computation (ABC), a widely adopted yet computationally demanding calibration technique. The core of the method relies on a supervised learning implementation of the Bidirectional Long Short-Term Memory (BiLSTM) neural network with an epidemiological soft constraint. Using our proposed method, we present

a comprehensive simulation study comparing both accuracy and efficiency between these methods.

Furthermore, we introduce **epiworldRCalibrate**, a software package implemented in the R programming language, which encapsulates our calibration approach and provides an accessible tool for researchers and practitioners. This paper proceeds by first presenting an overview of calibration methods in ABMs, followed by a detailed description of the proposed LSTM-based method, an extensive simulation study, and concludes with a discussion of findings and implications for future research.

2 Calibration in ABMs

Agent-Based Models (ABMs) are computational models in which individuals, or agents, are represented as unique and autonomous entities that interact with one another and with exogenous environments [10]. ABMs are powerful tools for exploring complex systems and can illuminate subjects such as regulation, investment, and banking activities where agents pursue specific goals. The three fundamental components of an ABM are the agents, the topology, and the environment. Agents are typically distinct in their characteristics and act independently, reflecting heterogeneity and autonomy. The topology specifies how agents are connected and interact, shaping the flow of information and influence within the system. Finally, the environment provides the external context in which agents operate. The overall behavior of the system emerges from the accumulative effects of individual agents and their interactions, often revealing dynamics that cannot be understood by analyzing agents in isolation. ABM calibration is a process used to refine and validate the ABM to approximate observed data as much as possible. Calibration involves adjusting various model parameters, such as agent attributes, decision-making rules, and environmental factors, to align the model’s behavior with empirical data or expert knowledge. Calibration requires comparing model outputs to observed data to identify the parameter values that best replicate real-world dynamics. There are various strategies for ABM calibration, namely, approximate Bayesian computation,^{11,3} simulated minimum distance,⁹ and surrogate models.^{5,4,12}

Approximate Bayesian Computation [ABC] avoids the need to compute the likelihood directly by comparing simulated model outputs with observed data using a distance metric, a great alternative when likelihood calculation is either computationally expensive or intractable. Using machine learning, Zhang, Li, Zhang, et al. [12] employs boosting to classify categorical data and enhance model generalization. Their method, CatBoost, modifies the gradient estimation in the classical algorithm, reducing the influence of estimation bias and improving performance. While such algorithms address predictive performance, recent de-

velopments in uncertainty quantification [UQ]² provide complementary tools for calibrating and analyzing complex simulation models.

Despite the advances in calibration techniques, some limitations persist, including the need for significant computational resources and the difficulty of handling high-dimensional and complex models. In other words, while ML applications have made calibration faster, simulation-based algorithms like Markov Chain Monte Carlo are still needed to infer the model parameters. Additionally, capturing the whole uncertainty landscape of parameter estimates and effectively incorporating heterogeneity among agents remain ongoing challenges.

3 Methods

3.1 Problem set up

SIR models are parametrized by the recovery rate (p_{recov}), basic reproduction number (R_0), transmission rate (p_{tran}), population size (N) and contact rate (c_{rate}), which combined with an initial number of infected cases (prevalence), can generate *epidemic* curves (epi_t), e.g. the stock of infected agents over time. More formally, an SIR model can be seen as a random map M_{SIR} from its parameters to its generated epidemic curves, i.e.

$$M_{SIR} : \theta \rightarrow Y, \quad (1)$$

with the specific mapping M_{SIR} being complex and unknown in reality, especially considering a wide range of θ values. Our task with this paper is to utilize the data Y generated by ABMs with varying parameters θ , to learn the inverse mapping

$$M_{SIR}^{-1} : Y \rightarrow \theta \quad (2)$$

in a supervised manner. A successful deployment of ML to learn M_{SIR}^{-1} would allow us to feed it observed disease data in Y , letting us: (i) recover the SIR fundamental parameters $\hat{\theta}$; and (ii) utilize $\hat{\theta}$ to understand the current epidemiological dynamics, such as predicting future number of cases.

3.2 Machine Learning Method: BiLSTM Model

The *calibration* task consisting in learning the map M_{SIR}^{-1} in (2) from epidemic trajectories to underlying parameters naturally calls for sequence models. *Recurrent neural networks*

(RNNs) are well suited to this setting because they maintain a hidden state that propagates information across time, allowing the model to encode the growth–peak–decay phases that characterize ABM-generated epidemic curves. Among RNN variants, we adopt a *Long Short-Term Memory* (LSTM) architecture because its gating mechanism (input, forget, output gates) mitigates vanishing gradients and preserves medium-range temporal dependencies over tens of days, which is essential for distinguishing parameter combinations that produce similar early dynamics but diverge near the peak or in the tail. We further use a *bidirectional* LSTM (BiLSTM) since calibration is performed on complete trajectories rather than streaming data; leveraging both forward- and backward-time context improves the identifiability of parameters from the full curve shape.

We train our specific BiLSTM model, defining its data input with what is typically observed for diseases: the population size, recovery rate and incidence curve. We task it to predict key epidemiological parameters: the transmission probability, contact rate, and the basic reproduction number. According to our problem set up in (2), this formally means:

$$Y := \{N, p_{\text{recov}}, \text{epi}_t\} \quad \text{and} \quad \theta := \{p_{\text{tran}}, c_{\text{rate}}, R_0\}, \quad (3)$$

where θ contains critical parameters for understanding and controlling epidemic outbreaks.

Alternative models. We considered simpler recurrent cells (e.g., vanilla RNNs or GRUs) and more complex attention-based encoders (Transformers). While GRUs are lighter, LSTMs offer a more expressive gating scheme that proved advantageous for our 30–60 day horizons. Transformers are state-of-the-art for long sequences and large training corpora, but in our application—short sequences, a low-dimensional target (3 parameters), and a modest data regime—they introduce substantial parameterization and training overhead without commensurate gains. BiLSTM therefore provides a parsimonious and effective compromise: it captures the relevant temporal structure of ABM incidence curves while remaining stable to train and straightforward to deploy.

We also explored Convolutional Neural Networks (CNNs) for our calibration task. While CNNs are typically used for images, we adapted them to time series by using 1D temporal convolutions and global pooling to map incidence trajectories directly to epidemiological parameters. However, our comparative analysis showed that BiLSTMs performed better on this sequential task because they are expressly designed to capture temporal dependencies across the growth–peak–decay phases of an epidemic curve. Beyond predictive performance, LSTM-based models also offered a practical advantage for our data pipeline: they handle variable-length trajectories cleanly via padding together with masking (or packed sequences), so padded time steps are ignored during training. This allowed us to ingest contagion curves

of differing lengths without truncation or ad hoc resampling, and thus we proceeded with BiLSTM networks for our calibration approach.

Input data. One of the great benefits of this approach is that the training data can be generated by the SIR model, with ABM simulations. Since the goal is to recover the model parameters from realized datasets within the model, we completely rely on data simulated from the ABM. Thus, the input to our model consists of daily incidence counts spanning sequences of typically 60 days, complemented by crucial known time-invariant covariates, namely population size and recovery rate (p_{recov}). For most diseases, p_{recov} is typically known, or could be reasonably estimated, although its inclusion in our model only improves R_0 prediction marginally, leaving unchanged p_{tran} and c_{rate} prediction accuracy. Our input covariates are normalized using MinMax scaling, facilitating machine model learning by ensuring inputs are on a comparable scale, and the same scalers were applied at test time. Details regarding the specific SIR data-generating process we utilized to train our BiLSTM are described in Appendix A.

Model architecture. We use three stacked BiLSTM layers with 160 hidden units each, a depth-width combination selected via hyperparameter tuning; making the network deeper or wider did not yield material gains. Bidirectionality lets the model exploit both past-to-future and future-to-past context in the full epidemic trajectory, improving identifiability of parameters from curve shape. Because this capacity is relatively high compared with our 30–60 day sequences, we regularize the inter-layer representations with dropout applied *between* LSTM layers (as in PyTorch’s `dropout` argument), which discourages co-adaptation while preserving the cell’s within-time memory dynamics. We tuned the rate over 0.10–0.50 and selected 0.5 by validation loss (Optuna), achieving a favorable bias-variance trade-off and mitigating overfitting; in effect, this behaves like averaging over thinned subnetworks and yields more stable estimates of transmission probability, contact rate, and R_0 from noisy incidence curves.

Output activation function. The final hidden states from the forward and backward directions of the BiLSTM layers are concatenated with the normalized time-invariant features, creating a rich and informative feature representation. This combined feature set is then passed through two fully connected dense layers: the first dense layer with 64 units employing a ReLU activation function to introduce non-linearity, followed by a final output layer designed to produce epidemiologically interpretable predictions.

Output layer activations are carefully selected to enforce biologically meaningful constraints: a sigmoid activation function bounds the transmission probability between 0 and 1, and softplus activation functions ensure positivity for the predicted contact rate and the basic reproduction number (R_0).

Training regime and loss function. Our training regime employs the *Adam* optimizer with a learning rate of approximately 2.77×10^{-4} , chosen via extensive Optuna-based hyperparameter optimization. The model is trained with a composite loss function \mathcal{L} comprising Mean Squared Error (MSE) and a penalty term designed to maintain epidemiological consistency. Specifically, the penalty encourages the predicted parameters to satisfy the theoretical relationship $R_0 \times \text{recovery rate} \approx \text{transmission probability} \times \text{contact rate}$. The loss function can be mathematically represented as:

$$\mathcal{L}(\phi) = \mathbb{E} \left[\underbrace{\|\hat{\theta}_\phi(Y) - \theta\|_2^2}_{\text{MSE term}} + \lambda \underbrace{(\hat{R}_{0,\phi}(Y) \gamma - \hat{p}_{\text{tran},\phi}(Y) \hat{c}_{\text{rate},\phi}(Y))^2}_{\text{epidemiological consistency penalty}} \right], \quad (4)$$

where $\theta = \{p_{\text{tran}}, c_{\text{rate}}, R_0\}$, $Y = \{N, p_{\text{recov}}, \text{epi}_t\}$, and ϕ are BiLSTM parameters.

We used a batch size of 64 and trained the model for up to 100 epochs, employing an early stopping criterion based on validation set performance to prevent overfitting and ensure computational efficiency.

Overall, this carefully designed approach not only ensures high predictive accuracy and computational efficiency but also guarantees epidemiological coherence in parameter estimation, making our model particularly suitable for real-time calibration and informing public health decision-making.

Furthermore, the implementation of this calibration method is publicly available on GitHub at <https://github.com/sima-njf/epiworldRcalibrate>.

4 Simulation Study

Our simulation study rigorously evaluates and benchmarks the performance of Approximate Bayesian Computation (ABC), particularly, the likelihood-free Markov Chain Monte Carlo (LFMCMC) algorithm,⁷ as implemented in the R package **epiworldR** package⁸ against a data-driven bidirectional Long Short-Term Memory (BiLSTM) estimator for parameter estimation and epidemic forecasting within the agent-based SIR modeling framework. Specifically, we executed a comprehensive set of simulations involving 1,000 independent parameter scenarios. For each scenario, we generated synthetic epidemic trajectories and subsequently assessed each method’s ability to recover underlying epidemiological parameters, accurately predict infection dynamics, and efficiently calibrate models.

The parameter values used to generate the testing datasets were the same as those we used for training the BiLSTM (see Appendix A). It is important to highlight two points: First, we use a new draw from the model parameters to generate the testing dataset, and

second, the prior distributions used to generate the training and testing sets are sufficiently wide to create highly heterogeneous realized epi curves.

The testing procedure consisted of comparing how well each method was at recovering (a) the parameter values used to generate the curve and (b) the curve itself. For each one of the 1,000 drawn parameters, we did the following:

1. Simulate a 60-day epidemic of daily infected counts using the agent-based SIRCONN model in the `epiworldR` package.
2. Each method was then used to calibrate the model to the generated infected counts. Calibration using our proposed method was done using the `epiworldRCalibrate` package, and ABC calibration was done using the implementation available in `epiworldR`.

After running the calibration procedure, we compared both parameter estimates and goodness of fit of the epi curves in the following ways:

Parameter recovery. For each method, we calculated bias, relative bias, and Mean Absolute Error of each parameter. Notwithstanding, parameter recovery is crucial for an inferential process. It is essential for the reader to note that our model’s primary objective is to reproduce the observed epi curve. Because of how the contact rate and transmission rate interact in the ABM, exactly recovering both of them is not possible. We further discuss this point later in the Discussion section of the paper.

Predictive bias. After estimating parameters with ABC, we forward simulate 100 new curves using the calibrated parameters and compare the predicted trajectories against those from the ground-truth parameters. This allows us to assess the downstream predictive performance of the calibrated parameters in realistic settings: $\Delta_t = I_t - \hat{I}_t$ and Δ_t/I_t . In addition to bias and relative bias, we also computed the empirical 95% credible-interval coverage, as well as computation time (wall-clock seconds per ABC and BiLSTM).

All the code used to conduct the experiment is available in the following GitHub repository: https://github.com/UofUEpiBio/Sims_calibrate.

5 Results: Comparing with ABM

5.1 Predictive Evaluation: ABC vs BiLSTM

We systematically assess the predictive accuracy of two distinct modeling approaches, Approximate Bayesian Computation (ABC) and Bidirectional Long Short-Term Memory (BiLSTM), in forecasting infectious disease dynamics under scenarios characterized by parameter

uncertainty. Each approach was rigorously tested using 1,000 distinct parameter sets, with each set evaluated through 100 stochastic simulations extending over a period of 60 days, ensuring comprehensive coverage of diverse epidemiological conditions and parameter configurations.

Figures below illustrate comparative predictive trajectories generated by ABC and BiLSTM models for infected individuals, cumulative infected, and susceptible populations. These figures include clearly marked 95% prediction intervals, highlighting variability and predictive confidence. Notably, the BiLSTM model consistently produces tighter and more precise credible intervals, signifying a superior capability to accurately forecast disease progression dynamics over the entire simulation horizon.

To illustrate this, we show a snapshot of the prediction interval bounds over time. Table 1 displays a subset of the daily lower and upper quantile values for predicted infection counts from day 0 to day 9. This comparison reveals both the increasing spread of the epidemic and the contrasting uncertainty estimates of the two models. BiLSTM’s narrower bounds suggest more confident and sharper estimates compared to the broader intervals seen in ABC outputs.

Table 1: Interval bounds for ABC and BiLSTM

Day	ABC_Q2.5	ABC_Q97.5	BiLSTM_Q2.5	BiLSTM_Q97.5
0	47.0	174.0	45.0	173.0
1	56.5	261.0	53.3	234.0
2	66.1	415.0	63.6	366.0
3	72.3	698.0	70.0	616.0
4	75.7	1064.0	74.3	1010.0
5	80.5	1592.0	78.5	1553.0
6	83.2	2231.0	82.9	2177.0
7	88.2	2906.0	86.7	2766.0
8	92.9	3455.0	91.4	3375.0
9	96.9	3656.0	96.4	3532.0

These findings demonstrate that the BiLSTM model is not only more efficient but also better calibrated, offering a more reliable predictive envelope for public health decision-making. The visual and numerical evidence points to BiLSTM’s advantage in uncertainty quantification, which is crucial for scenario planning in rapidly evolving epidemiological contexts. These plots provide further insight into the differences in predictive uncertainty between ABC and BiLSTM. Figure 2 compares the bias and coverage performance of the ABC and BiLSTM methods for epidemiological parameter estimation using simulated in-

Table 2: Detailed summary of estimation error metrics for epidemiological parameters by ABC and BiLSTM methods.

Parameter	Method	MAE	RMSE	Mean Bias	Median Bias
R_0	ABC	0.275	2.840	0.0784	-0.00646
	BiLSTM	0.0616	0.0825	0.0168	0.0108
Contact rate	ABC	4.240	5.930	4.070	3.240
	BiLSTM	1.020	1.220	-0.489	-0.464
Transmission Rate	ABC	0.128	0.187	-0.121	-0.0821
	BiLSTM	0.0715	0.0975	0.000348	0.0227

fected count data. The top-left panel shows the mean percentage bias over the 60-day period, with BiLSTM maintaining near-zero bias while ABC exhibits substantial negative bias, particularly between days 10 and 20. The top-right panel shows coverage over time, with both methods remaining close to the nominal 95% coverage level. The bottom-left panel summarizes key statistics, indicating that BiLSTM achieves lower mean absolute bias and RMSE compared to ABC. The bottom-right panel compares overall coverage, showing both methods achieve values close to the 95% target, though BiLSTM provides consistently more accurate predictions with reduced bias.

Figure 3 illustrates the performance of the BiLSTM model in predicting transmission probability (p_{tran}), contact rate (c_{rate}), and basic reproduction number (R_0) from ABM-generated epidemiological time-series data. Predicted values are plotted against actual values, with the red dashed line indicating the ideal 1:1 correspondence. The model achieves low prediction errors for p_{tran} (MAE = 0.0577) and R_0 (MAE = 0.0572), demonstrating strong agreement with the true values. However, predictions for c_{rate} show substantial bias and reduced accuracy (MAE = 0.9892), indicating challenges in learning contact rate dynamics from the available input features.

5.1.1 Parameter Recovery Accuracy

Accurate parameter estimation is critical in epidemiological modeling, influencing the robustness and utility of predictive models. We evaluated the ability of ABC and BiLSTM methods to recover key epidemiological parameters by analyzing their estimation errors. Table 2 provides a detailed summary of the performance metrics.

Also, Table 3 presents the average wall-clock time required to perform a single model calibration run for both the Approximate Bayesian Computation (ABC) and the Bidirectional Long Short-Term Memory (BiLSTM) methods.

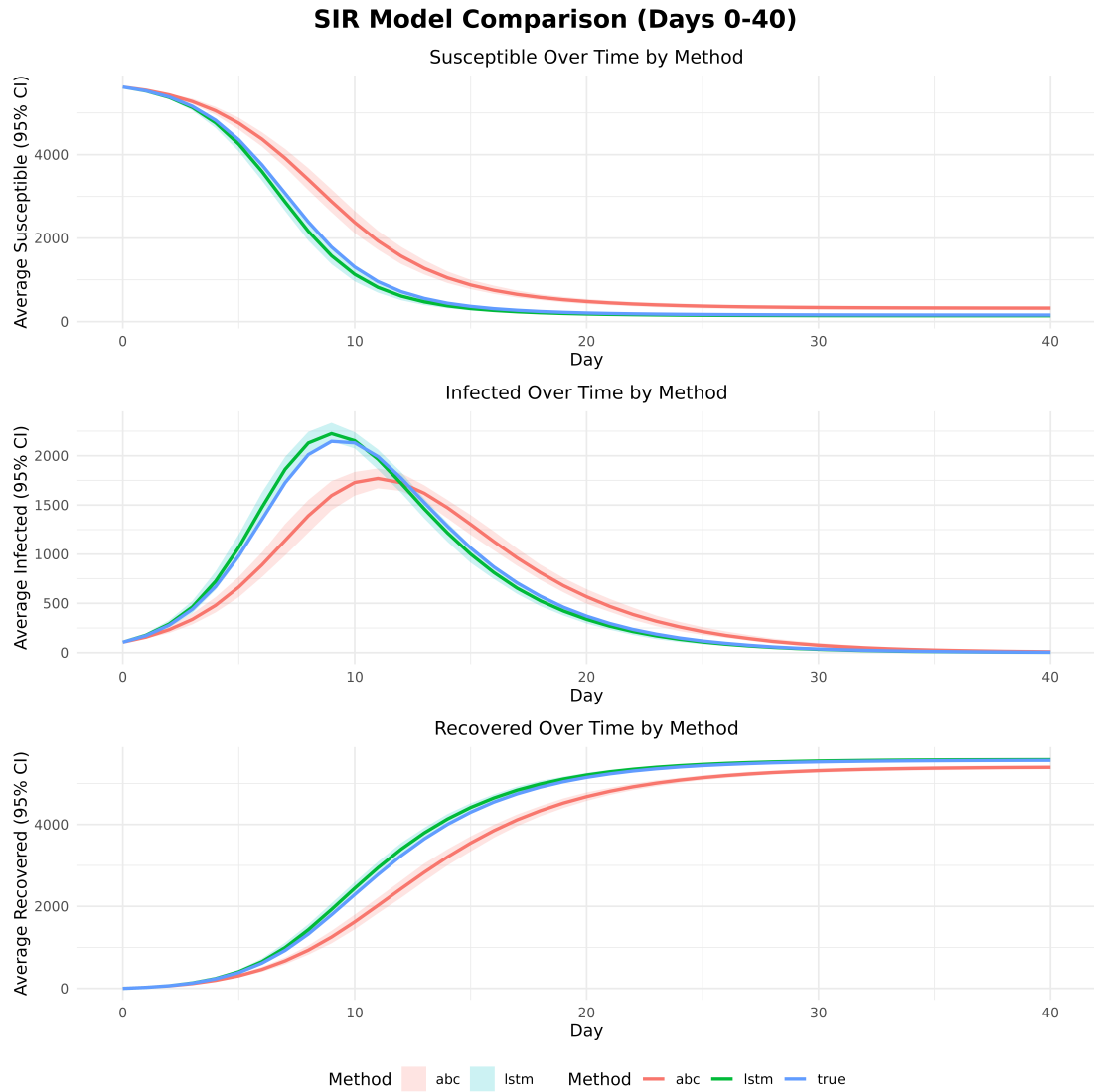


Figure 1: Predicted epidemic curves showing susceptible, infected, and recovered populations over 40 days for a representative subset of parameter simulations. Credible intervals indicate model uncertainty.

Table 3: Wall-clock time per calibration run for ABC vs. BiLSTM methods.

Method	Computation Time
Approximate Bayesian Computation (ABC)	77.40 seconds
Bidirectional Long Short-Term Memory (BiLSTM)	2.35 seconds

Bias and Coverage Analysis: ABC vs LSTM Methods

1000 Parameter Sets \times 100 Runs Each \times 60 Days | Infected Counts

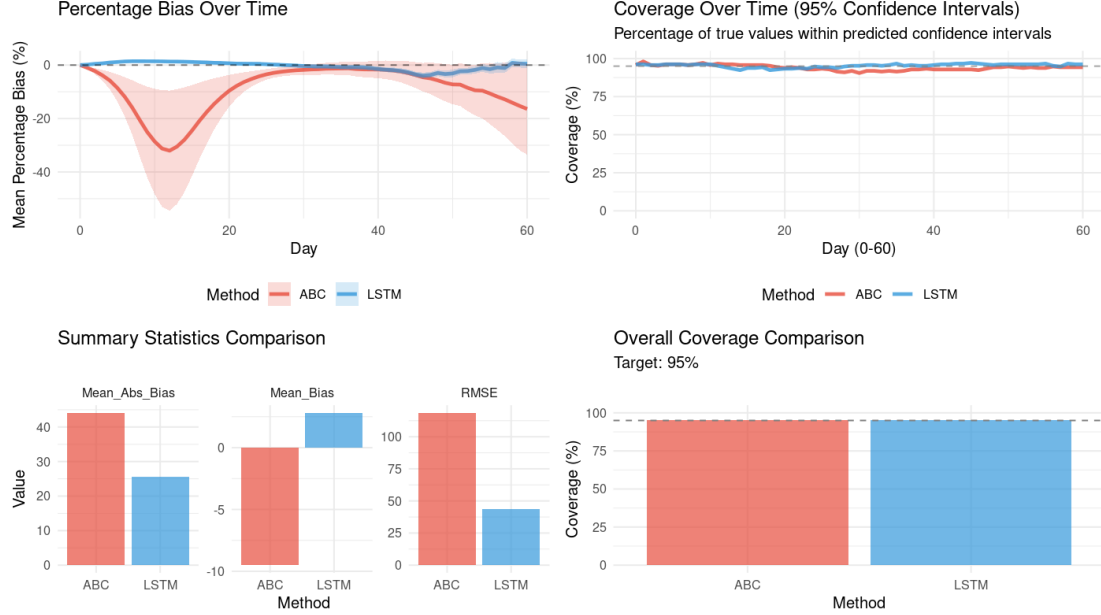


Figure 2: Comparative analysis of predictive bias and coverage between ABC and BiLSTM methods over a 60-day forecast period. The BiLSTM model consistently demonstrates lower bias and superior coverage accuracy.

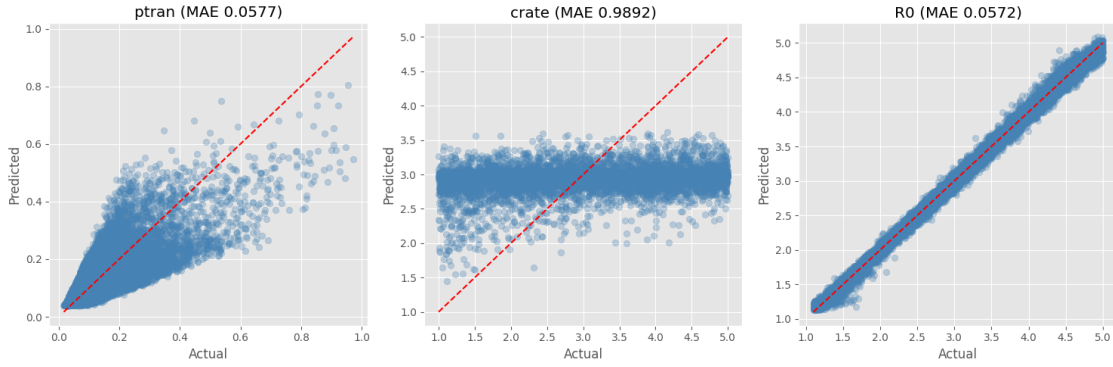


Figure 3: Performance of the BiLSTM model trained on ABM-generated epidemiological time-series data in predicting transmission probability (p_{tran}), contact rate (c_{rate}), and basic reproduction number (R_0). Scatter plots compare predicted versus actual values for each parameter, with the red dashed line indicating the ideal 1:1 correspondence. The Mean Absolute Errors (MAEs) are reported in parentheses for each metric.

Figure 4 provides a visual comparison of the bias distribution for each parameter estimated using ABC and BiLSTM methods. The plots combine violin and boxplot representations, offering both distribution shape and summary statistics such as median and quartiles.

Across all three parameters, BiLSTM demonstrates a consistently narrower spread in

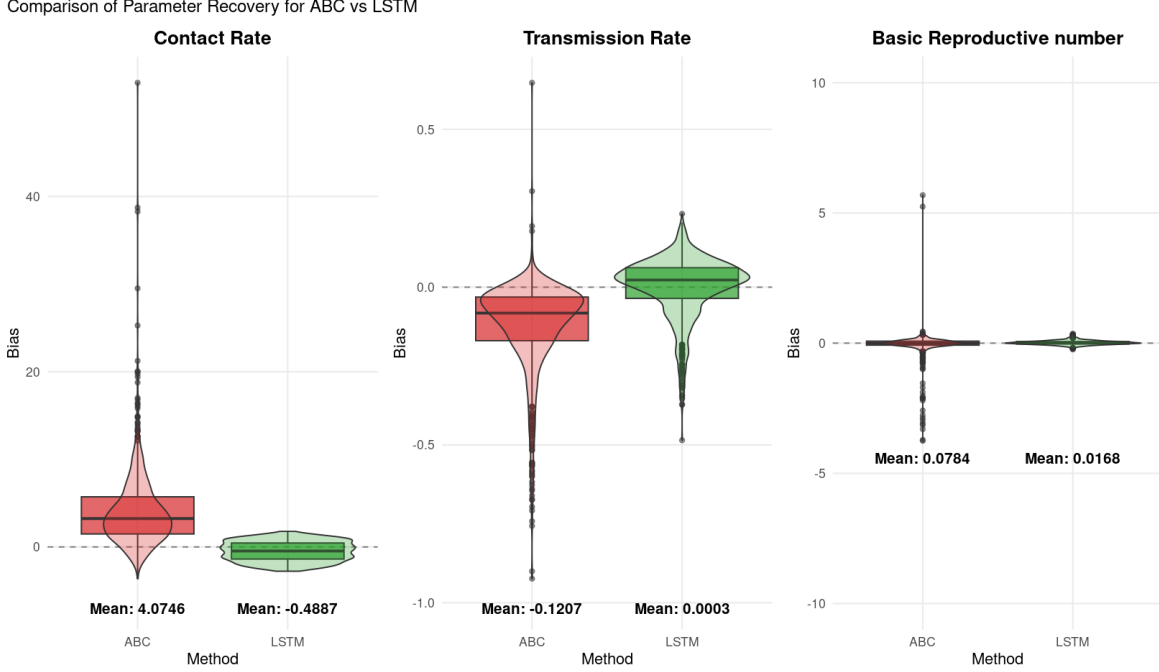


Figure 4: Violin and box plots showing the distribution of parameter estimation bias for ABC and BiLSTM methods across three key epidemiological parameters: Contact Rate, Transmission Rate, and Basic Reproduction Number (R_0).

the distribution of bias, and its median bias is closer to zero. This reflects both improved central accuracy and lower variability. For instance, in the case of the contact rate, ABC exhibits a long right tail—indicating the tendency to substantially overestimate in certain scenarios—whereas BiLSTM remains tightly centered with less skew. Similarly, for transmission probability and R_0 , the BiLSTM model again shows tighter concentration of estimates around the true values.

Collectively, these results underline the substantial advantages of the BiLSTM method in predictive accuracy, parameter recovery, and computational efficiency compared to traditional ABC methods in modeling infectious disease dynamics. The tight predictive intervals, improved estimation accuracy, and computational scalability make BiLSTM an especially compelling option for real-time applications, such as outbreak forecasting and public health intervention planning.

6 Discussion

In this study, we introduced and rigorously evaluated the ML Calibration Framework framework, a novel approach designed to calibrate agent-based models (ABMs) efficiently and

accurately. This framework leverages machine learning, specifically a bidirectional Long Short-Term Memory (BiLSTM) neural network, alongside Approximate Bayesian Computation (ABC) to achieve fast, reliable, and scalable parameter estimation. Our comprehensive simulation study, encompassing 1,000 simulated epidemic scenarios, clearly demonstrates the strengths of the ML Calibration Framework approach compared to traditional ABC calibration methods.

A critical observation emerging from our analysis is the inherent challenge in simultaneously identifying the three parameters—contact rate, recovery rate, and transmission rate—with high precision, even with sophisticated machine learning architectures and increased data volume. This difficulty arises because at least one parameter tends to default to its average estimate, suggesting a fundamental identifiability constraint within the SIR model framework. Notably, this limitation does not significantly affect the practical utility of our predictions, as the calibrated parameters still produce accurate epidemic curves. This outcome implies that the underlying dynamics of incidence curves generated by SIR models may effectively possess only two degrees of freedom, reinforcing the notion that accurate incidence predictions can be made without precisely estimating every individual parameter. Although in our framework the parameters θ (contact rate, recovery rate, transmission rate) function primarily as nuisance parameters—estimated only as a means to generate reliable epidemic curves—it is still possible to quantify uncertainty in their values. Future work could extend our calibration framework to incorporate statistical inference on θ , for instance, by generating distributions of predicted parameter sets rather than single point estimates. One practical approach would be to train multiple calibrators on bootstrapped datasets (e.g., 100 models), thereby producing a collection of plausible parameter estimates. This ensemble-based strategy would enable the construction of credible intervals for θ , providing additional insight into parameter uncertainty while preserving the predictive focus of our modeling.

Our evaluation revealed several distinct advantages of the ML Calibration Framework. First, the BiLSTM neural network substantially improved parameter recovery accuracy compared to ABC-only methods. Specifically, the BiLSTM approach resulted in lower mean absolute error and root-mean-square error across all targeted parameters, with error distributions consistently centered around zero and exhibiting minimal dispersion. In contrast, ABC methods demonstrated broader error distributions, heavier tails, and systematic biases, particularly evident in parameters such as contact rate and R_0 .

Second, the predictive performance of the ML Calibration Framework was superior. Epidemic trajectories derived from BiLSTM-calibrated models consistently showed reduced bias and narrower 95% prediction intervals, while maintaining coverage rates near the nominal 95%. This indicates that the BiLSTM method achieves a more precise yet reliable forecasting

capability compared to ABC.

Third, computational efficiency represented a notable strength of our proposed framework. BiLSTM-based calibration completed within seconds on standard processors without parallel computing requirements, in sharp contrast to ABC-LFMCMC methods that necessitated over 11 minutes even with significant parallelization. This dramatic reduction in computational time significantly enhances the practical applicability of our approach, especially in real-time epidemic forecasting scenarios or situations requiring simultaneous evaluations across multiple settings.

One of the major benefits of employing a neural network for inverse modeling lies in its single-training requirement. After initial training, the model can rapidly produce parameter estimates and associated uncertainty intervals through a simple forward pass. Unlike ABC methods, which demand extensive simulation for each parameter exploration, our BiLSTM effectively exploits learned patterns from historical simulations. Additionally, neural networks excel at capturing complex nonlinear interactions among parameters, an essential feature for accurately modeling disease dynamics that often challenge traditional statistical sampling methods.

Looking forward, extending the ML Calibration Framework to accommodate real-world datasets, which frequently exhibit variable-length or streaming infection trajectories, is a promising direction. Enhancing the BiLSTM architecture with masking layers or attention mechanisms could enable the model to selectively process observed data segments, thereby improving robustness and flexibility in real-world surveillance and response contexts.

In conclusion, the ML Calibration Framework represents a substantial advancement in ABM calibration, offering notable improvements in accuracy, efficiency, and computational practicality. Our results strongly advocate for its adoption in epidemiological modeling and potentially other domains reliant on simulation-based model calibration and parameter estimation. The integration of machine learning with traditional Bayesian methods significantly transforms the calibration landscape, facilitating real-time, large-scale applications and informed decision-making in complex modeling scenarios.

7 Conclusions

Agent-based models (ABMs) have become indispensable tools across diverse scientific fields, particularly in public health, where they enable detailed scenario modeling of disease outbreaks. Despite their widespread application, calibrating ABMs remains computationally intensive, necessitating the development of methods to expedite the process and improve accuracy. Existing approaches typically rely on surrogate modeling to approximate the ABM,

thereby creating a direct mapping from model parameters to observed outcomes.

In this paper, we introduced an innovative method that reverses this paradigm, constructing an inverse mapping directly from observed data to model parameters. Demonstrating the utility of our approach, we implemented it using a Bidirectional Long Short-Term Memory (BiLSTM) neural network, trained exclusively on simulated data. This allowed us to develop a generalized learner capable of accurately calibrating an SIR-type ABM across various epidemiological scenarios.

Through a comprehensive simulation study, we benchmarked our approach against Approximate Bayesian Computation (ABC), a widely used but computationally demanding calibration technique. Results indicated that our method consistently outperformed ABC, achieving superior accuracy in recovering true model parameters and epidemic curves, while significantly reducing computational demands. Our methodology has been encapsulated in the `epiworldRcalibrate` R package, making it readily accessible for practical use.

Nevertheless, significant challenges remain. Issues such as parameter identifiability and the extension of our approach to more complex models, including mixing models and SEIR frameworks, require further investigation. Addressing these challenges presents promising avenues for future research, potentially extending the applicability and impact of ABM calibration methods in public health and beyond.

8 Acknowledgments

This work was made possible by cooperative agreement CDC-RFA-FT-23-0069 from the CDC’s Center for Forecasting and Outbreak Analytics. Its contents are solely the responsibility of the authors and do not necessarily represent the official views of the Centers for Disease Control and Prevention.”

References

- [1] Claudio Angione, Eric Silverman, and Elisabeth Yaneske. “Using Machine Learning as a Surrogate Model for Agent-Based Simulations”. In: *PLoS ONE* 17.2 (2022), e0263150. DOI: 10.1371/journal.pone.0263150.
- [2] Claudio Angione, Eric Silverman, and Elisabeth Yaneske. “Using Machine Learning as a Surrogate Model for Agent-Based Simulations”. In: *PLOS ONE* 17.2 (Feb. 2022). Ed. by Roland Bouffanais, e0263150. ISSN: 1932-6203. DOI: 10.1371/journal.pone.0263150. (Visited on 07/17/2023).

- [3] Nicolò Gozzi et al. “Preliminary modeling estimates of the relative transmissibility and immune escape of the Omicron SARS-CoV-2 variant of concern in South Africa”. In: *medRxiv* (2022), pp. 2022–01.
- [4] Hawre Jalal, Thomas A. Trikalinos, and Fernando Alarid-Escudero. “BayCANN: Streamlining Bayesian Calibration With Artificial Neural Network Metamodeling”. In: *Frontiers in Physiology* 12 (2021), p. 662314. ISSN: 1664-042X. DOI: 10.3389/fphys.2021.662314.
- [5] Francesco Lamperti, Andrea Roventini, and Amir Sani. “Agent-Based Model Calibration Using Machine Learning Surrogates”. In: *Journal of Economic Dynamics and Control* 90 (May 2018), pp. 366–389. ISSN: 01651889. DOI: 10.1016/j.jedc.2018.03.011. (Visited on 12/01/2022).
- [6] Francesco Lamperti, Andrea Roventini, and Amir Sani. *Agent-Based Model Calibration using Machine Learning Surrogates*. 2017. arXiv: 1703.10639 [q-fin.EC]. URL: <https://arxiv.org/abs/1703.10639>.
- [7] Paul Marjoram et al. “Markov Chain Monte Carlo without Likelihoods”. In: *Proceedings of the National Academy of Sciences of the United States of America* 100.26 (Dec. 2003), pp. 15324–15328. ISSN: 00278424. DOI: 10.1073/PNAS.0306899100. pmid: 14663152. URL: www.pnas.org/cgi/doi/10.1073/pnas.0306899100.
- [8] Derek Meyer and George G Vega Yon. “epiworldR: Fast Agent-Based Epi Models”. In: *Journal of Open Source Software* 8.90 (Oct. 3, 2023), p. 5781. ISSN: 2475-9066. DOI: 10.21105/joss.05781. URL: <https://joss.theoj.org/papers/10.21105/joss.05781> (visited on 10/04/2023).
- [9] Donovan Platt. “A comparison of economic agent-based model calibration methods”. In: *Journal of Economic Dynamics and Control* 113 (2020), p. 103859.
- [10] Steven F. Railsback and Volker Grimm. *Agent-Based and Individual-Based Modeling: A Practical Introduction*. 2nd ed. Princeton, NJ: Princeton University Press, 2019. ISBN: 9780691190839.
- [11] Tina Toni et al. “Approximate Bayesian Computation Scheme for Parameter Inference and Model Selection in Dynamical Systems”. In: *Journal of The Royal Society Interface* 6.31 (July 9, 2008), pp. 187–202. DOI: 10.1098/rsif.2008.0172. URL: <https://royalsocietypublishing.org/doi/full/10.1098/rsif.2008.0172> (visited on 07/30/2025).

- [12] Yi Zhang, Zhe Li, Yongchao Zhang, et al. “Validation and calibration of an agent-based model: A surrogate approach”. In: *Discrete Dynamics in Nature and Society* 2020 (2020).

A Simulation of Parameters and Data

A.1 Parameter Setup

All parameters are randomly drawn for each simulation as follows:

$$\begin{aligned}
 N \text{ (population size)} &\sim \text{Uniform}(5000, 10000), \\
 p_{recov} \text{ (recovery rate)} &\sim \text{Uniform}(0.071, 0.25), \\
 \text{Prevalence} &\sim \frac{\text{Uniform}(100, 2000)}{N}, \\
 R_0 &\sim \text{Uniform}(1, 5), \\
 c_{rate} \text{ (contact rate)} &\sim \text{Uniform}(5, 15), \\
 p_{tran} \text{ (transmission rate)} &= \frac{R_0 \cdot p_{recov}}{c_{rate}} \quad (0 \leq p_{tran} \leq 1).
 \end{aligned}$$

Table 4 summarizes these distributions.

Table 4: Parameter setup for training scenarios.

Parameter	Description	Distribution / Value
N	Population size (known)	Uniform(5000, 10000)
Recovery rate	Recovery rate (known)	Uniform(0.071, 0.25)
Prevalence	Initial infected proportion	Uniform(100,2000)/N
Contact rate	Effective contacts per person	Uniform(5,15)
R_0	Basic reproduction number	Uniform(1,5)
Transmission rate	Transmission probability per contact	$R_0 \times p_{recov}/c_{rate}$

A.2 Preparation of Incidence Data

Each simulated scenario yields a 60-day infected-count trajectory. We transform it into a 1×60 array:

- daily incidence (new infections).

Table 5 defines these rows.

Table 5: Structure of the data array for each scenario.

Row	Description
1	Daily incidence (new cases each day)

B ABC details

The ABC procedure focuses on estimating three key parameters: contact rate, recovery rate, and transmission rate, while keeping prevalence and R_0 fixed during calibration. Since the model we are simulating is fairly simple, here we use the entire simulation outcome as the target statistic. More details about the implementation of the algorithm can be found in Appendix B

Each LFMC MC chain runs for 2,000 iterations. The first 1,000 are discarded as burn-in, and the posterior median of the accepted samples is used as the point estimate.

- **Observed data:** For each simulation, we generate a 60-day trajectory of infected counts using true parameters. This serves as the reference data for calibration.
- **Forward simulator:** We define a function `simulate_epidemic_calib()` that simulates a 60-day epidemic given a set of candidate parameters and returns the daily counts of infected individuals.
- **Summary statistic:** The full time series (identity function) is used directly, retaining maximum information without dimensionality reduction.
- **Parameter proposal mechanism:** At each iteration, new candidate parameters are proposed using the following transformations:

$$\begin{aligned} c'_{rate} &\leftarrow c_{rate} \cdot e^{\mathcal{N}(0, 0.1^2)}, \\ p'_{recov} &\leftarrow p_{recov} \cdot e^{\mathcal{N}(0, 0.1^2)}, \\ p'_{trans} &\leftarrow \text{logit}^{-1}(\text{logit}(p_{trans}) + \mathcal{N}(0, 0.1^2)). \end{aligned}$$

- **Discrepancy measure:** The similarity between simulated and observed trajectories is measured using Euclidean distance. The kernel weight assigned to a proposed parameter set is:

$$K_\varepsilon = \exp\left(-\frac{\|S' - S_{\text{obs}}\|_2^2}{2\varepsilon^2}\right), \quad \varepsilon = 0.05 \cdot \|S_{\text{obs}}\|_2,$$

where S' is the simulated series and S_{obs} is the observed one.